



Study of the hygroscopic properties of three Australian wood species used as solid wood and composite products

Maryam Shirmohammadi¹

Received: 12 January 2023 / Accepted: 16 May 2023 / Published online: 17 July 2023
© Crown 2023

Abstract

The use of engineered wood products and mass timber panels such as cross laminated timber (CLT), glued laminated timber (glulam) and laminated veneer lumber (LVL) is becoming more common, as these products have benefits in terms of environmental credentials and resource utilisation and have the potential to provide faster and more economical construction processes. However, timber exposed to moisture for prolonged periods can degrade biologically, leading to a loss of appearance and decreased mechanical properties. Southern pine, radiata pine and shining gum timber are important forest resources for the Australian timber industry. To date, no in-depth studies on the hygroscopic properties of these species have been carried out from a timber wetting point of view. Consequently, existing literature has a knowledge gap regarding the determination of moisture movement properties in these species that are applicable to numerical modelling when used as solid wood or in the production of engineered wood products (EWPs). The work presented herein will help develop a better understanding of moisture ingress and egress in solid timber and EWPs and provide data for future predictive tools (such as numerical modelling) for moisture management in timber buildings. Samples were prepared from solid timber as well as EWP's to examine the relationships between glue lines and edge gaps in CLT and multiple glue lines in LVL on moisture movement. As expected, longitudinal permeability was higher than radial and tangential permeability for the species tested. Southern pine samples had higher gas and liquid permeability values than radiata pine and shining gum. CLT with end grain sections including an edge gap had higher gas and liquid permeability than similar sections with glue lines only. LVL sections with 1 glue line had slightly lower permeability values than in samples with 2 glue lines. Gas and liquid permeabilities were lower for LVL samples than a two-layered veneer section without a glue line illustrating the barrier posed by the glue line. The moisture loss parameter during the diffusion testing was higher for LVL ends and CLT ends with edge gaps than face and edge sample sections. The results will be used to develop numerical models for moisture behaviour in solid and composite timber panels when exposed to humidity and free water. It is recommended to conduct additional studies to examine the impact of the adhesive layer and its properties on impeding moisture migration or functioning as a moisture barrier.

List of symbols

Symbol	Description (Unit)
D_a	Apparent density (kg/m ³)
D_t	True density (kg/m ³)
\emptyset	Porosity (%)
K	Intrinsic permeability (m ²)
Q	Flux (m ³ s ⁻¹)
μ	Dynamic viscosity (Pa)

✉ Maryam Shirmohammadi
maryam.shirmohammadi@daf.qld.gov.au

¹ Queensland Department of Agriculture and Fisheries, Brisbane, Australia

Symbol	Description (Unit)
e	Sample thickness (m)
P	Pressure (Pa)
ΔP	Pressure difference between air inlet and outlet
\bar{P}	Average pressure inside sample
A	Sample area (m ²)
D_b	Diffusion coefficient through wood
m	Mass (kg)
L	Sample thickness (m)
t	Time (s)
G	Specific gravity at moisture content (kg/m ³)
ρ_w	Density of water (kg/m ³)

Symbol	Description (Unit)
X	Moisture content (%)
ΔX	Moisture variation between two parallel faces of the sample
M_t	Mass loss (g/m)

1 Introduction

Timber and timber composite systems offer substantial benefits, including very low embodied energy, good insulation properties and more economical construction processes when compared to other building materials. As a biological material, however, timber products can absorb and desorb moisture from the environment. Due to their hygroscopic nature the wetting and drying cause changes in the sample structure including dimensional instability, aesthetic degrade and fungal decay. Poorly designed or maintained timber products may also be affected by prolonged exposure to moisture that can cause product degradation, performance loss and failure. The rate and extent of damage can vary, depending on the exposure environment of the products (Viitanen 1994, 1998; Viitanen et al. 2010; Isaksson et al. 2013; Brischke and Alfredsen 2020; Libralato et al. 2021a, b). Moisture intrusion into solid timber or mass panel composites, and cyclic variation in moisture during and post construction could cause changes in appearance and structural properties that can be difficult to repair. Southern pine (*Pinus elliottii* x *Pinus caribaea*) (SP), radiata pine (*Pinus radiata*) (RP) and shining gum (*Eucalyptus nitens*) (SG) are three commercially available species in Australia. There have been various studies (Tumer and Perré 1995; Turner 1996; Perré and Turner 1999a, b; Redman et al. 2016, 2017; Redman 2017) focusing on the properties of wood during drying. However, the movement of water in these three species during periodic and long-term wetting when exposed to free water still requires further research. Specifically, the effects of anatomical differences between species (cell type, density variations and structure differences) as well as variations between solid timber products and EWP (including layered structure, glue lines, gaps between the boards and glue types) need to be addressed (Gereke et al. 2009a, b, 2010). The differences between species and the effects of their anatomical characteristics (such as pore size/types, permeability, chemistry and cell size) on moisture movement over time are important when long-term durability and structural stability of products are estimated (Popper et al. 2009; Redman et al. 2012, 2017; Taghiyari and Avramidis 2019; Jang et al. 2020). Additionally, the hygroscopic properties will enable the comparison between EWPs made from different species for better building material selection, design for preventing moisture damage and maintenance/monitoring specifications. The hygroscopic properties of the three

species, when used as solid timber and EWPs, require investigation to elucidate the effects of solid wood properties and the structure (change in direction of boards, cell arrangement of veneers), glue lines, edge gaps, cracks, and other features of EWPs. These factors are important when specifiers use these panels in their building service life estimates (MacKenzie et al. 2007; Schmidt et al. 2019; Quesada-Pineda et al. 2020; Shirmohammadi and Leggate 2020; Chang et al. 2021; Bucklin et al. 2022). Moisture ingress into solid wood and EWPs could occur due to poor site management during erection, poor building design, types of construction or poor maintenance (Beebe and Kam-Biron 2016). Knowledge of species differences, and effects of composite structure on moisture movement characteristics of EWPs will enable building practitioners to implement appropriate protocols, special care plans and maintenance processes in scenarios where repeated moisture exposure occurs during the construction and post-construction service life of products (Beebe and Kam-Biron 2016). In addition to the complexity of moisture ingress and egress scenarios for EWPs, there is also need for further research relevant to long-term performance aspects of these components when used in the wide variety of Australian environments in which timber is employed (e.g. higher decay hazard situations) (Franke et al. 2016; Niklewski et al. 2018). This paper discusses porosity, density, permeability and diffusivity measurements of solid timber (sawn timber) from three Australian species and Australian conifer mass timber panels.

2 Materials and methods

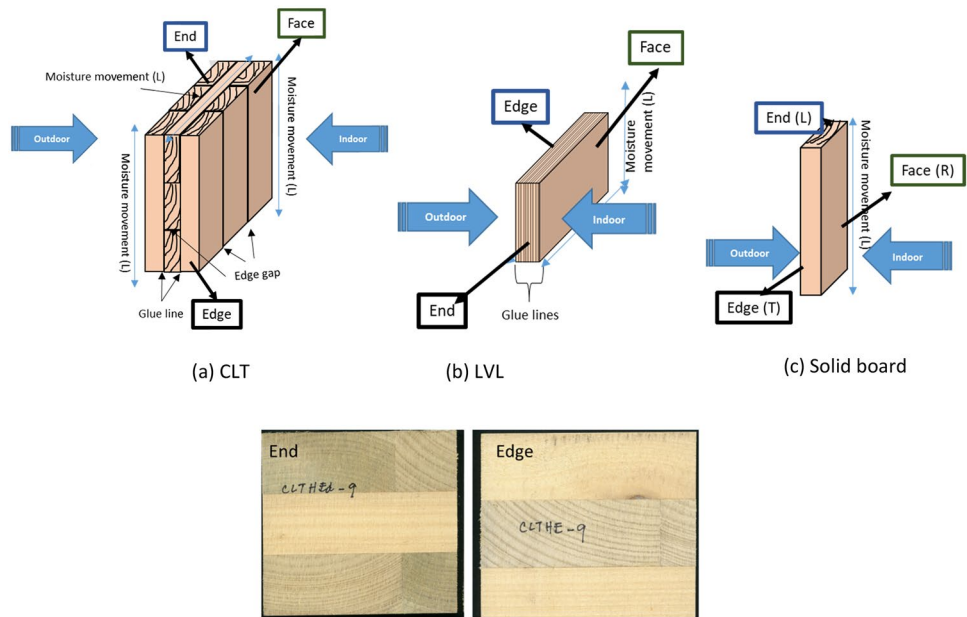
2.1 Samples

Solid timber samples (sawn timber) of southern pine, radiata pine, and shining gum, radiata pine cross laminated timber (CLT) (by Xlam, Australia) and *Pinus* laminated veneer lumber (LVL) (purchased from local suppliers, Brisbane, Australia) were used to determine moisture movement properties. Before testing, samples were conditioned at 25 °C and 65% relative humidity (RH) to approximately 12% equilibrium moisture content (EMC). Initial sample dimensions were determined. Figure 1 shows the direction of focus in the study for moisture movement properties on solid timber boards and EWP panels. Face, edge and end were selected to examine the effects of exposure direction of the sample on moisture movement.

2.2 Density and porosity

For individual boards and the constituent species of panels, the pore size and shape for the species influence the moisture movement properties (Redman 2017; Tibebe 2021). Density

Fig. 1 Direction of water movement examined in the panels (a and b) and boards (c) that were monitored. CLT end and edge directions showing end-grain proportions (d)



and porosity were measured on sample blocks nominally 20×20×20 mm conditioned at 25 °C and 65% RH. The conditional requirements were followed according to AS/NZS 1080.3:2000 (Australia 2016). For each category of sample, five replications were tested. Samples with specific characteristics were cut from EWP panels to fit the test apparatus. This included CLT samples containing two pieces of timber orthogonal to one another with a glue line in between (2Piece/2P) and similar samples that had a single piece on one side of the glue line and two pieces on the other side with a non-edge-glued gap in between (3Piece/3P) (Fig. 2B and C).

Each sample was weighed, and its dimensions measured (Table 1). Pore size and porosity were studied on samples cut from the face, end, and edge directions (Fig. 1). For pine, the proportion of the earlywood (EW) and latewood bands (LW) was recorded.

Apparent density uses the volume of the piece including void space and was calculated using Eq. 1, where D_a is apparent density of samples (kgm^{-3}). For true or voidless density (D_t) samples were placed in a gas pycnometer and density was recorded 5 times and averaged for data analysis.

$$D_a = \frac{\text{Mass}(\text{kg})}{\text{Volume}(\text{m}^3)} \tag{1}$$

Sample’s porosity was calculated using the true and apparent density values. The porosity of samples (\varnothing in %) was calculated using Eq. 2.

$$\varnothing = \left(1 - \left(\frac{D_a}{D_t} \right) \right) \times 100 \tag{2}$$

2.3 Permeability

The gas and liquid permeability of the three solid timber species, CLT, and LVL composite panels were determined in the laboratory. Gas and liquid permeability were measured using a POROLUX 1000 prometer (IB-FT GmbH, Berlin, Germany) (Redman et al. 2017; Manh et al. 2022). For gas permeability, samples were tested with pressurised air until the pressure reached the 4000 millibars. For liquid permeability, non-distilled water was applied to the sample surface with a pressure at constant level of 4000 millibars. The permeability values were determined using Darcy’s law (Eq. 3):

$$K = \frac{Q\mu eP}{A\Delta P\bar{P}} \tag{3}$$

In this equation, K is the intrinsic permeability (m^2); Q is the volume flux ($\text{m}^3 \text{s}^{-1}$); μ is the dynamic viscosity of air (Pa); e is the sample thickness (m); P is the pressure at which flux Q is measured (Pa); A is the sample area (m^2); ΔP is the pressure difference between the air outlet and inlet sides of the sample (Pa); and \bar{P} is the averaged pressure inside the sample (Pa). Samples (8–10 mm thick) were cut along the radial, tangential and longitudinal pathways using a 24 mm diameter hole-saw (Fig. 3). Ten replicates were tested per sample type and direction. Water movement into the side

Fig. 2 Sample blocks used for porosity and density measurement (A boards, B CLT-2P, C CLT-3P and D LVL)

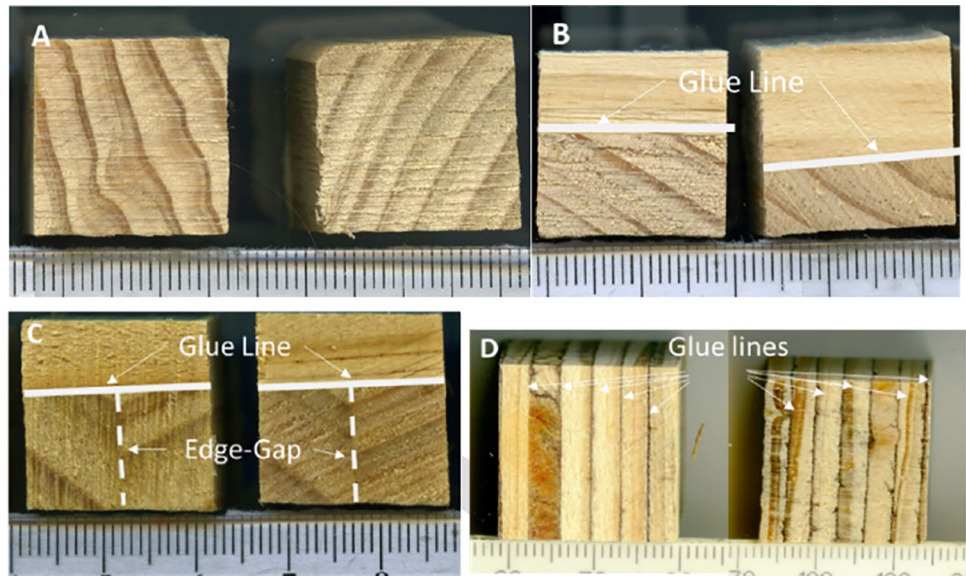
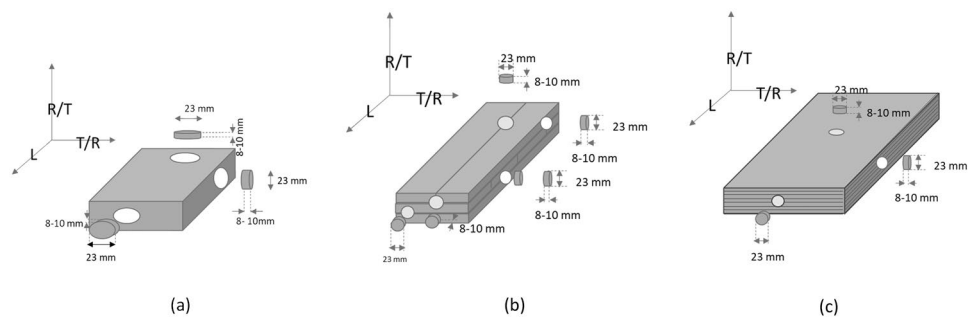


Table 1 Average mass and dimensions of samples used for measuring density and porosity

Sample	Length (mm)	Width (mm)	Height (mm)	Weight (g)
Southern pine (low % LW)	19.92 ± 0.18	20.00 ± 0.11	19.84 ± 0.23	4.19 ± 0.25
Southern pine (high % LW)	19.92 ± 0.15	19.93 ± 0.3	19.78 ± 0.3	4.92 ± 0.35
Radiata pine (low % LW)	20.07 ± 0.12	19.83 ± 0.1	19.89 ± 0.18	4.20 ± 0.09
Radiata pine (high % LW)	19.23 ± 0.79	19.94 ± 0.17	19.91 ± 0.11	4.86 ± 0.29
Shining gum	19.76 ± 0.3	19.98 ± 0.5	20.27 ± 0.45	4.72 ± 0.2
LVL	20.41 ± 0.22	20.73 ± 0.2	20.54 ± 0.22	5.98 ± 0.24
CLT-3 P	19.97 ± 0.07	19.99 ± 0.35	19.98 ± 0.48	4.04 ± 0.13
CLT 2 P	19.86 ± 0.18	19.98 ± 0.21	19.91 ± 0.24	4.10 ± 0.1

± Values are the standard deviation

Fig. 3 Preparing samples for permeability tests in the different directions for boards (a), CLT (b) and LVL (c) panels



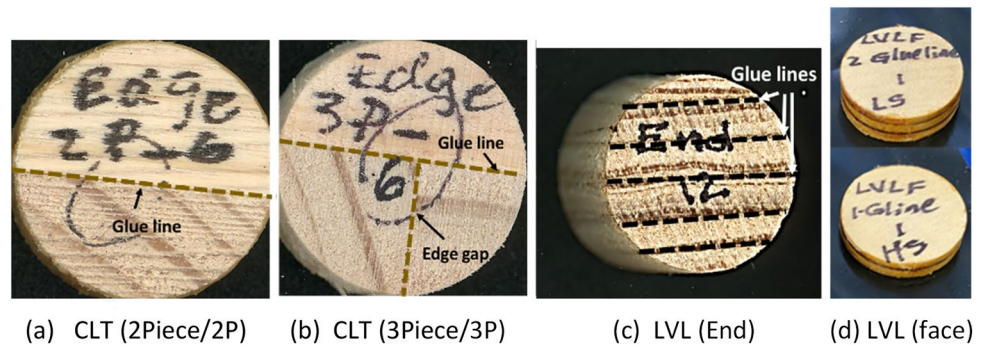
surfaces of the sample was restricted by the application of two layers of epoxy resin (Redman 2017).

For LVL and CLT samples, sections with edge gaps and glue lines were cut to determine the effects of these features on permeability values. Sample sections were cut according to the diagrams shown in Fig. 4.

The effects of the number of glue lines on liquid and gas permeability in LVL samples were assessed on samples

with 1 and 2 glue lines, with piece thicknesses of 4–5 mm and 7–8 mm respectively. One veneer layer (average thickness of 3.7 ± 0.16 mm) or two veneer layers (average thickness of 3.7 ± 0.17) without a glue line in between were also tested to investigate the effects of the glue line as a potential water barrier. All testing conditions were repeated eight to ten times and samples were prepared from sections with no damage, knots or visible cracks.

Fig. 4 Sample sections. **a** CLT (2Piece/2P). **b** CLT (3Piece/3P). **c** LVL (End). **d** LVL (face)



2.4 Diffusivity

Diffusivity of wood sections was determined by exposing different sides of samples to varying levels of humidity. Five to ten replications were tested for each sample type. The vaporimeter technique as shown in Fig. 5 was used to investigate steady-state water vapour diffusivity (Redman et al. 2017; Manh et al. 2022). Samples for end grain and edge measurements were prepared with similar dimensions as used for permeability testing. Face (radial direction) samples of the three species were prepared with a larger diameter to capture the water vapour diffusivity in a larger cross Sect. (74 mm diameter). The two different humidity conditions applied on each side/large face of the samples were dry and saturated. Vaporimeters used for the experiments were similar to the PVC-CHA system developed by AgroParisTech (Agoua et al. 2001).

Samples were conditioned to 65% RH and 25 °C temperature prior to testing. The circular sections were then placed in similar diameter glass containers filled with a saturated solution of sodium chloride (> 99.9%) in deionized/purified water. Cylindrical PVC was used to seal the samples in place and cable ties were used to fix the PVC in place (Fig. 5). The samples were then placed in a climatic chamber set to produce 9% EMC (23 °C and 50% RH). The two different humidity conditions (high saturation on one side and drier

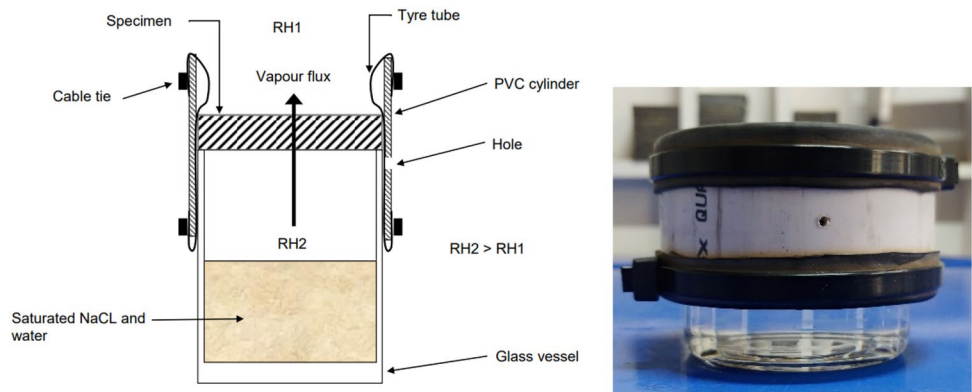
condition on the other side) created a diffusion flux through the sample thickness. The mass variation of samples was recorded over time. The diffusion coefficient through wood (D_b) was then calculated using Eq. 4.

$$D_b (m^2 \cdot s^{-1}) = \frac{mL}{tAG\rho_w\Delta X} \tag{4}$$

where m is mass of vapour transferred in kg, L is specimen thickness in meters, t is time in seconds, A is specimen surface area in m^2 , G is specific gravity at moisture content X (determined at approximate MC of 12% or conditioned at 25 °C and 65% RH), ρ_w density of water in kgm^{-3} and ΔX is the moisture variation between the two parallel faces of samples in kg/kg (the data was taken from Author’s current research project on moisture sorption and desorption). The ΔX is calculated as the average moisture content of the sample’s bottom and top faces.

The effects of sample geometry (the differences between sample dimensions in transverse, longitudinal and radial directions) in comparing the diffusivity data were minimised by determining the mass loss parameter as shown in Eq. 5, where M is the mass loss in g, A is the surface area in m^2 and L is the sample length in m (Redman et al. 2017). The mass loss values were determined as

Fig. 5 Testing set-up used for diffusivity determination (image taken from previous work as modified by Redman (2017))



$$M_l = \frac{M}{A} \times L \tag{5}$$

For CLT and LVL samples, sections of face, edge and end directions were prepared for diffusivity measurements. The sections had glue lines and edge gaps in order to monitor the effects of composite structure on movement of water vapour through the sections.

2.5 Statistical analysis

The data collected were statistically analysed using Analysis of Variance (ANOVA) ($\alpha=0.05$) to investigate the effects of different variables on moisture properties of samples tested. The differences between the means of experimental data were assessed using Tukey’s HSD ($\alpha=0.05$). The parameters that had significant effect on output values were reported in each section. GenStat (Genstat 2022) was used for all the statistical analysis.

3 Results and discussion

3.1 Porosity

Results of porosity measurements for the three species are shown in Fig. 6. The porosity values determined for radiata pine and southern pine samples (Fig. 6a and b) with a higher percentage of latewood (radiata pine: $43\% \pm 9$ and southern pine: $54\% \pm 6$) were lower than samples with a higher percentage of earlywood (radiata pine: $72\% \pm 6$ and southern pine: $76\% \pm 64$). Shining gum samples showed lower porosity values than southern pine and radiata pine samples.

The density values showed the difference between the true and apparent density of samples as a result of the effects of voids (Table 2). The true density values determined for composite sections were lower than the apparent density values due to the gaps and glue line in the structure. The

Fig. 6 Porosity measurement versus density for three species of solid timber and CLT and LVL sections, **a** average values for solid radiata and southern pine samples and **b** values of porosity and density for radiata and southern pine samples with high and low percentages of early wood

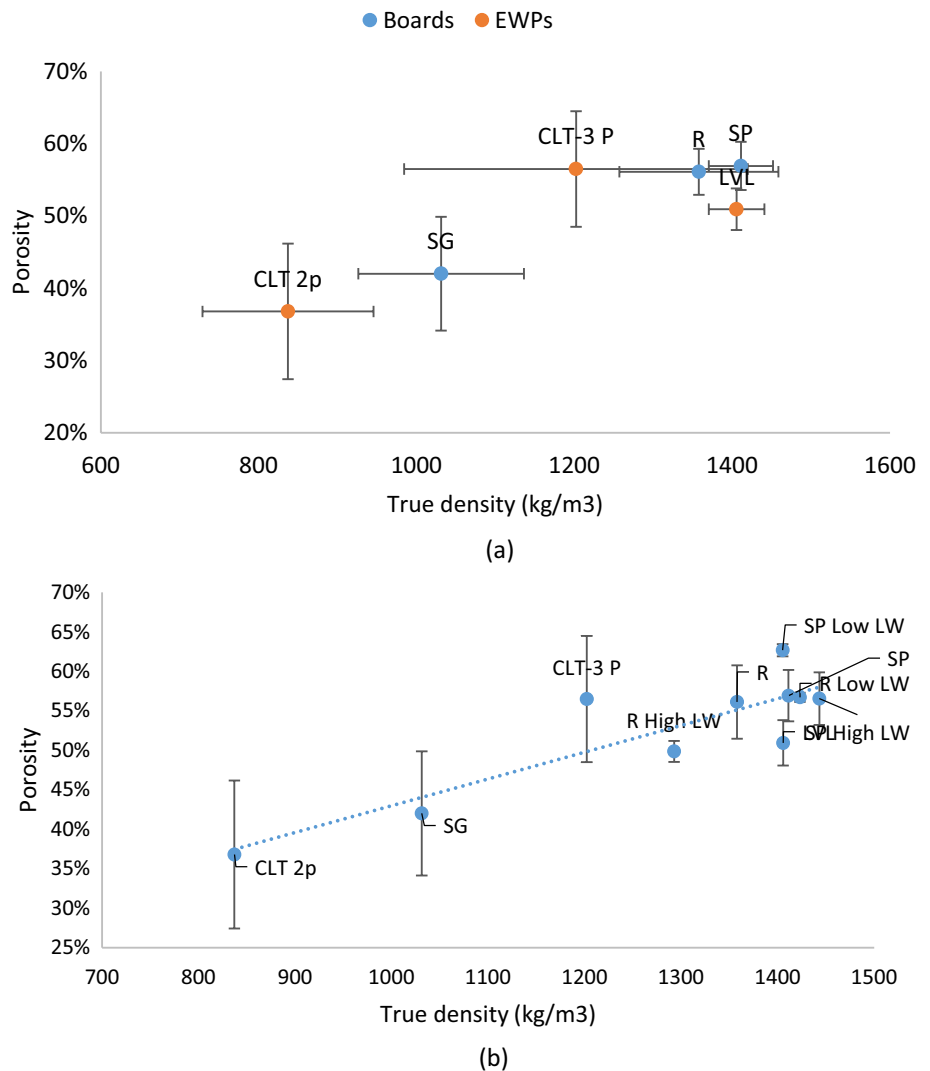


Table 2 Average apparent and true density determined for samples tested

	Apparent density (Kg/m ³)	True density (Kg/m ³)
Southern pine (High % LW)	627 ± 45	1443 ± 41
Southern pine (Low % LW)	531 ± 35	1405 ± 40
Southern Pine average	608 ± 40	1411 ± 71
Radiata pine (low % LW)	531 ± 11	1423 ± 13.3
Radiata pine (high % LW)	636 ± 32	1293 ± 188
Radiata pine average	584 ± 22	1358 ± 101
Shining gum	590 ± 32	1031 ± 105
CLT-3 P	506 ± 12	1202 ± 218
CLT 2p	519 ± 17	837 ± 108
LVL	689 ± 23	1406 ± 35

± are standard deviations

LVL true density however was higher than CLT and radiata pine (high LW %) and shining gum which could relate to the densification due to pressure gluing and compaction of layers/pores (Gaff et al. 2016). These structural effects need to be considered when density and porosity measurements are used in modeling building material response to the environment and for building service life calculations.

The CLT 3P sections (with glue line and edge gap) had higher porosity values than CLT 2P samples. The average porosity value for solid radiata pine samples was similar but slightly lower than the porosity of CLT 3P (made from radiata pine) and higher than CLT 2P. Considering the porous structure of timber and differences between solid samples and laminated structure of CLT, it is important to highlight the effects of glue line and edge gaps in porosity values for building design and moisture uptake preventions pre- and post-structure. The CLT 2P section with a glue line had a lower porosity (37%) than solid radiata pine samples that had an average porosity of 56%. The differences observed show the effect of glue line in reducing the porosity values of the 2P sections. The porosity value for LVL samples was lower than the average value for southern pine solid samples.

Schmidt and Riggio (2019) and Schmidt et al. (2019) investigated the performance of CLT building sections during construction of a three-story mass timber building. Their study outcomes indicated the need for detailed management of moisture, specifically in areas with a higher possibility of moisture accumulation and intrusion. Design should focus on minimising contact between the porous materials, specifically where end grain is exposed to potential high humidity or moisture and minimising moisture trapping by designing drainage and required spacing for air circulation (Schmidt and Riggio 2019; Schmidt et al. 2019). The

determined values of porosity and the anatomical images taken in this study indicate the need for further research focused on the effects of glue line, glue type and glue bond formation on moisture transfer in wetting and drying of mass timber products.

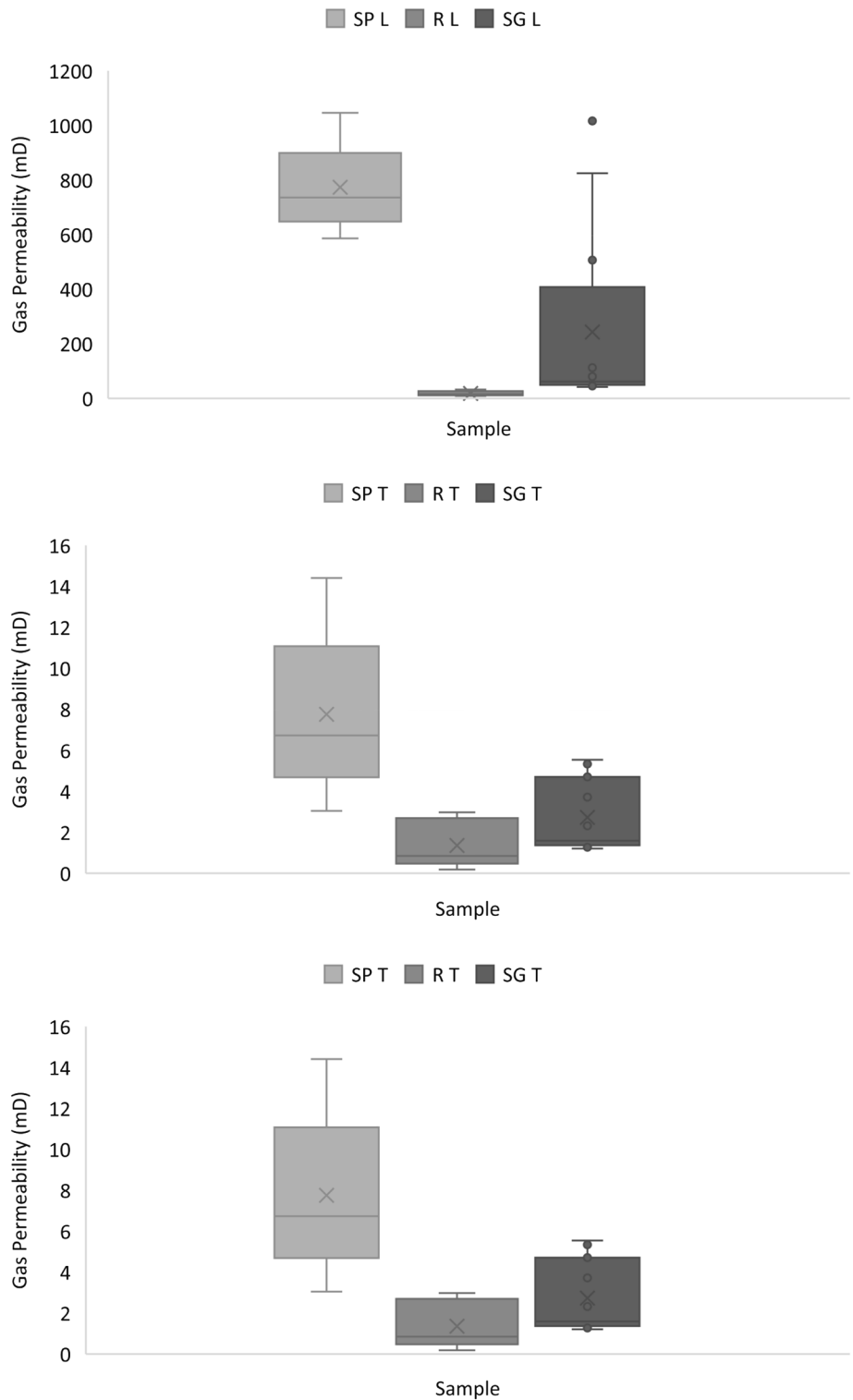
An ANOVA of porosity, apparent density and true density values of the low and high percentages of latewood in radiata pine significantly affected apparent and true density and porosity values. ANOVA on radiata and CLT sections showed that the sample type (radiata low LW, radiata high LW, CLT 3P and CLT 2P) significantly affected porosity, apparent and true density values.

3.2 Permeability (solid wood)

Wood is an anisotropic material where longitudinal permeability is significantly higher than in the other directions (more than 10⁶ times in case of hardwood) (Redman et al. 2012; Rivera Ramos et al. 2021; Manh et al. 2022). As expected, the gas and liquid permeability results for solid wood were higher in the longitudinal direction than in the tangential and radial directions for the three species (Redman et al. 2012, 2016; Redman 2017). Shining gum showed the highest variability in gas permeability data in the longitudinal direction. The gas permeability values determined for shining gum were close to zero in the radial direction and very low in the tangential direction (Fig. 7). Longitudinal gas permeability for shining gum samples was slightly higher than for radiata pine, considering the lower liquid uptake of shining gum than radiata pine; these results need to be investigated further in the future. Southern pine samples had the highest longitudinal gas permeability.

A higher ratio of gas permeability anisotropy was observed for shining gum in K_L/K_R than radiata or southern pine samples (Table 3). The longitudinal to tangential liquid permeability ratio (K_L/K_T) was much higher for shining gum in comparison to southern pine and radiata pine. The longitudinal to tangential gas permeability ratio (K_L/K_T), however, was higher for southern pine and shining gum and lower for radiata pine. The anisotropic nature of timber permeability for different species has been reported for different species previously (Comstock 1970; Turner 1996; Tanaka et al. 2010). These ratios indicate the force required for movement of liquid and gas that affect the hygroscopic properties of timber boards and composites when they are exposed to free water, as well as repeated wetting and drying leading to a moisture gradient inside the structure of the product (Friquin 2011). The anisotropic ratios could influence the scale of wetting and drying processes and lead to dimensional changes and internal stresses that are critical factors, especially in CLT connection design and maintenance (Redman et al. 2012; Taghiyari and Avramidis 2019; Jang et al. 2020). The ratios (K_R/K_T) were much lower for

Fig. 7 Gas permeability values for the three species tested, (SP is southern pine, R is radiata pine, SG is shining gum and L, R and T refer to longitudinal, radial and tangential directions)



both gas and liquid permeability values in the radial to tangential direction than K_L/K_T and K_L/K_R and shining gum had lower values in comparison to the pine samples. The high K_L/K_T value for southern pine was caused by the very low permeability in the tangential direction.

Liquid permeability of southern pine samples was higher in the longitudinal direction in comparison to radiata and shining gum samples (Fig. 8). Shining gum had the lowest radial and tangential liquid permeability, while radiata pine samples had the lowest longitudinal liquid permeability. The

Table 3 Anisotropy ratios of sample permeability values determined for solid timber of three species

Species	Permeability	K_L/K_R	K_L/K_T	K_R/K_T
Southern pine (SP)	Gas	29.65	99.80	3.37
	Liquid	202.66	1396.53	0.00071
Radiata pine (R)	Gas	5.48	13.25	2.42
	Liquid	16.46	233.62	0.0043
Shining gum (SG)	Gas	159.35	88.88	0.56
	Liquid	–	7579	0.00013

± Values are the standard deviation

small cell size arrangement of shining gum (Rivera Ramos et al. 2021) in comparison to the softwood samples could be one of the reasons for the lower permeability rates. However, the effects of extractive content in blocking vessels and resin content also need to be considered when permeability of these species is reported (Redman et al. 2012). Another study on the effects of wood type such as heartwood, intermediate wood, sapwood of hinoki, Douglas fir and hemlock showed significant effects of pore size, porosity and bulk density on gas permeability (Jang et al. 2020).

Southern pine samples had the highest longitudinal liquid and gas permeability compared to other species tested (Fig. 9).

3.3 Permeability (EWPs)

The CLT 3P samples had higher liquid permeability than the solid and 2P sections (Fig. 10). The 3P sections had an edge gap and glue line exposed to free water, while 2P sections only had a glue line exposed. Gaps between edges of boards have been considered influential factors in unequal wetting and drying of CLT sections in previous studies (Kukk et al. 2017, 2019a, b). Previous studies on wetting of mass timber panels in laboratory conditions have shown higher rate of moisture gain in the longitudinal fibre direction in comparison with the radial direction on the panel face (Liisma et al. 2019; Schmidt and Riggio 2019; Schmidt et al. 2019; Olsson 2020). Similarly, lower air leakage has been observed for edge-glued CLT samples compared to non-edge-glued CLT sections tested for their air permeability values. Püssa (2017) showed lower air permeability values for edge-glued samples compared to samples with open edge gaps. Samples exposed at lower RH's had more air-leakage for both edge-glued and open edged samples than in higher RH. Average air leakage of panels with open edges was 24% higher than the edge glued samples (Püssa 2017). A similar trend was observed when permeability data for CLT 2P and 3P sections were compared in the present study (Figs. 11 and

12). The observation illustrates how the behaviour of different elements of the composite CLT structure can influence longer-term performance if they are not considered in product maintenance and monitoring programs during construction and in the post-construction phases.

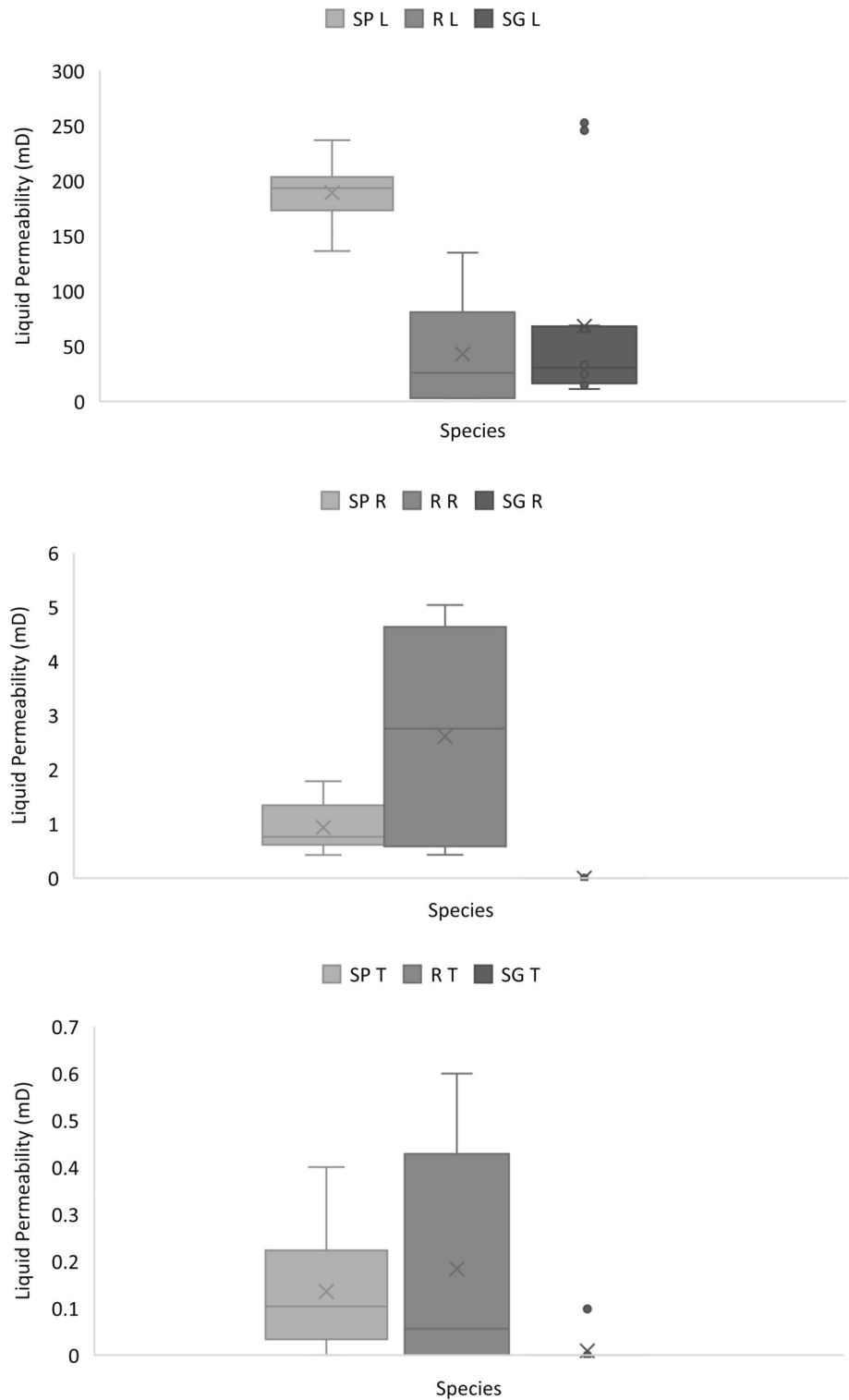
Higher gas permeabilities were recorded for 3P samples with the glue line and edge gap in comparison with 2P samples that only had the glue line in their structure (Table 4). The results illustrate the important effects of the non-edge glued gap on permeability which can result in accelerated moisture intrusion leading to more conducive conditions for fungal attack.

Permeability values for LVL sections were slightly lower for samples with two glue lines (gas permeability: 20.43 ± 13.3 and liquid permeability: 0.63 ± 1.1) than samples with one glue line (gas permeability: 28.8 ± 17.3 and liquid permeability: 1.21 ± 1.1). Samples of two veneer layers with no glue line showed higher liquid (23.1 ± 11.7) and gas (145.6 ± 57) permeability in comparison with sections with 1 and 2 glue lines (Table 5). Previous studies on LVL samples of *Populus tremuloides* (quaking aspen) with a phenol formaldehyde (PF) glue type showed that the net contribution of glue lines in gas permeability values of LVL sections was low (Wang and Ge 2016). The effects of veneer cell arrangement, glue line characteristics and glue type/specifications are some further factors that need to be considered when the permeability of LVL sections is investigated.

Light microscopic images of CLT and LVL sections (Fig. 13) show the glue line shape, thickness and penetration patterns. The section of CLT glued with polyurethane (PUR) glue showed glue penetration into earlywood bands, latewood bands and rays of radiata pine (Fig. 13). The 3P section of CLT with the edge gap and glue line also showed penetration of glue into the gap between the boards.

There were no visible air-bubbles in the phenol formaldehyde (PF) glue lines of the LVL samples as well as evidence of glue penetration into the micro-cracks on the veneer surfaces. PF resins are thermosetting and would not be expected to contain air-bubbles. In contrast, CLT glue-lines contained gas bubbles. The formation of air bubbles in the PUR glue line in the CLT sections was due to the release of carbon dioxide during curing and has been reported by other authors (Mohd Yusof et al. 2019; Sofi et al. 2021). The effects of species and wood cell orientation of boards on gas and liquid permeability were tested using an ANOVA. As expected, species and orientation both had significant effects on gas and liquid permeability ($\alpha=0.05$). Sample type (1P, 2P and 3P) had significant effects on both gas and liquid permeability while only gas permeability differed significantly between End and Edge samples.

Fig. 8 Liquid permeability data for species (SP: southern pine, R: radiata pine and SG: shining gum) tested in R: radial, T: tangential and L: longitudinal directions

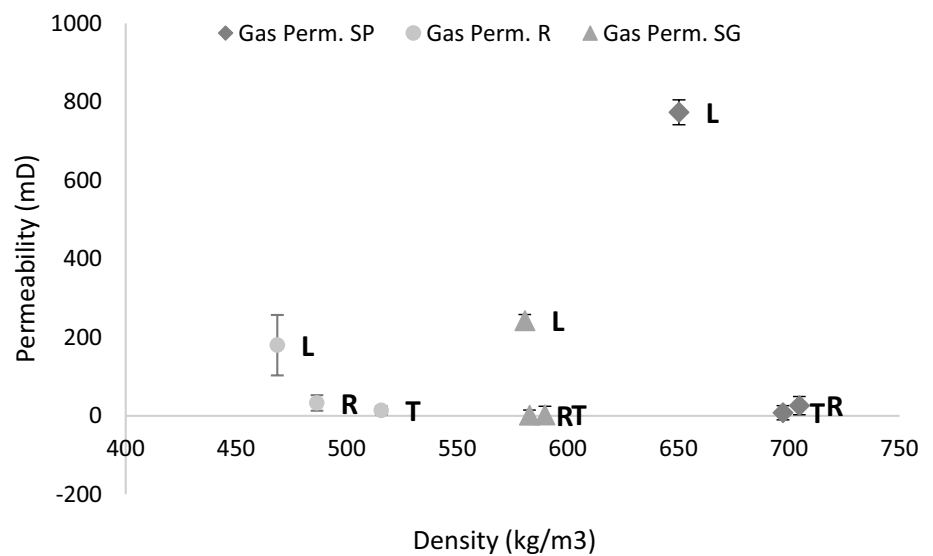


3.4 Diffusivity

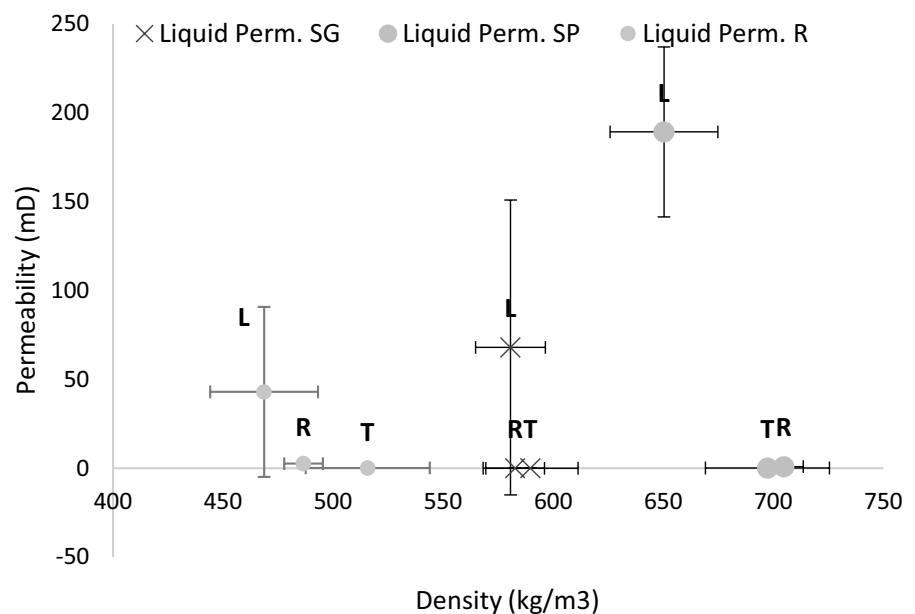
Diffusivity was evaluated on samples of the three species in three different directions by exposing sample sections to

high humidity conditions on one side and low humidity on the other. Figures 14 and 15 show samples' moisture variation when moisture diffusion is recorded through the sample thickness at 23 °C and 50% RH. The solid board samples had

Fig. 9 Summary of **a** gas and **b** liquid permeability data for southern pine (SP), radiata pine (R), and shining gum (SG) (On data points: L indicates longitudinal permeability, R indicates radial permeability, T indicates tangential permeability)



(a)



(b)

higher moisture gain in the longitudinal direction than in either the radial and tangential directions, which is consistent with the differences in permeability.

The LVL samples showed much higher moisture variations, which could reflect differences in glue line consistency or veneer layup patterns.

The CLT face sections reached lower moisture values in comparison with the end and edge section illustrating the effects of glue line as a water barrier. A similar trend was observed by Öberg and Wiege (2018) when modelling the differences between the solid timber and CLT.

The same approach of comparing the solid timber data was not applicable possibly due to variation in cell direction (veneer layer) and the presence of microcracks (peeler checks) in the veneers, glue type and veneer thickness.

Figure 16 shows the mass losses for boards and panel samples in different directions. The effects of different sample dimensions on diffusion were normalised by measuring changes in mass divided by the cross section of the sample multiplied by the sample thickness (Redman et al. 2012, 2017). The differences in graphs (Fig. 15) for longitudinal, tangential, and radial direction indicates the differences in water vapour

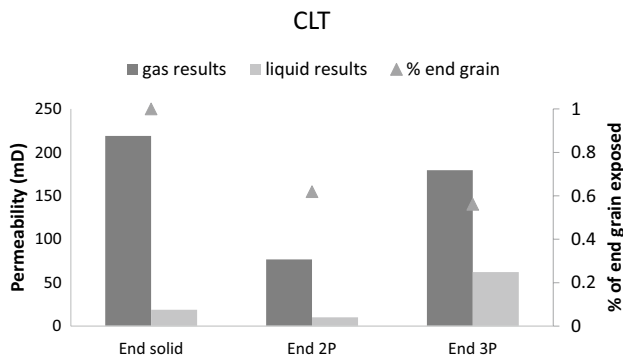
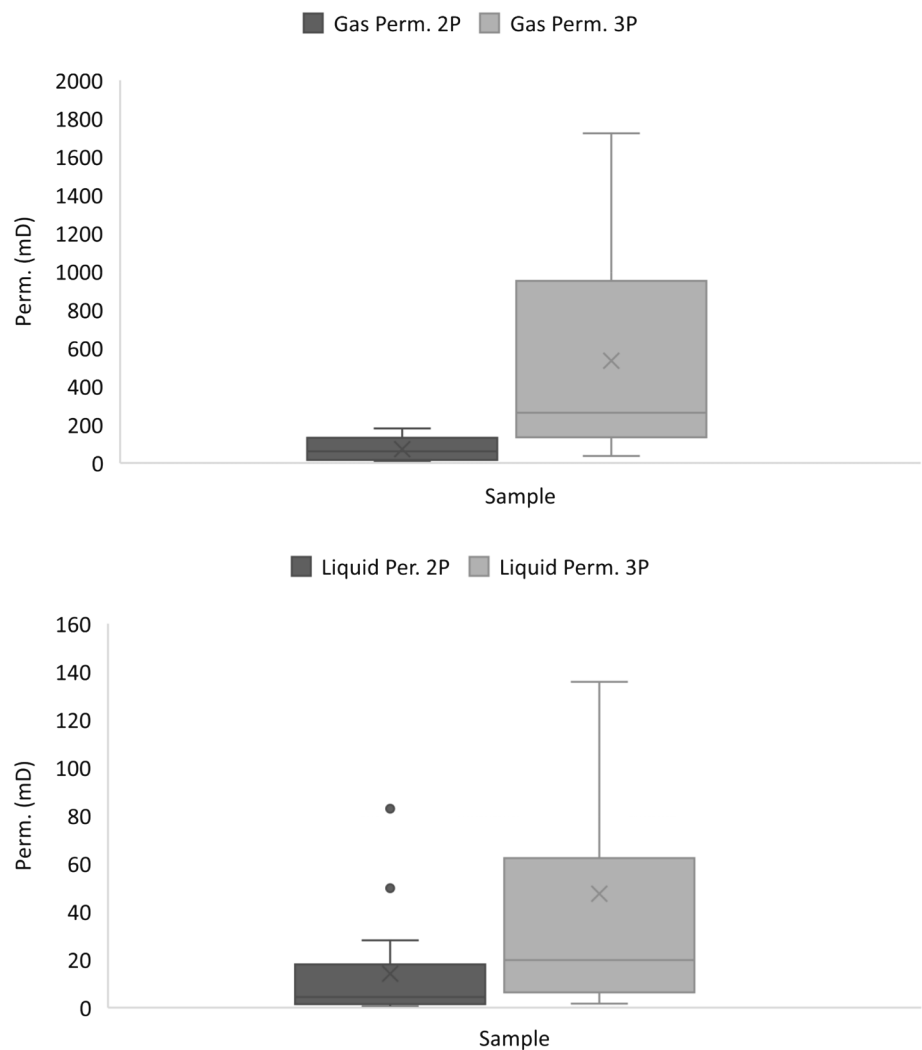


Fig. 10 Relationship between % of end-grain exposed on a CLT section and permeability

flux. Anatomical differences and chemistry of each species would be expected to influencing moisture flux (Redman et al. 2012, 2017).

Fig. 11 Average gas and liquid permeability values recorded for CLT 2P and 3P sections



Diffusivity of composite samples showed a more complex relationship with edges for 3P and 2P sections showing a higher mass loss in comparison with the CLT end sections. The diffusion coefficients for the CLT 2P section were higher (Table 6) in the three directions (end, edge and face) compared to the board values for all three solid timber species (Chiniforush et al. 2019). The relationship between diffusivity, temperature and moisture content studied on glulam made from pacific teak (*Tectona grandis*), Tasmanian oak (*Eucalyptus regnans/obliqua/delegatensis*), radiata pine (*Pinus radiata*), slash pine (*Pinus elliotii*) or blackbutt (*Eucalyptus pilularis*), CLT made of Norwegian spruce (*Picea abies*), and LVL made of radiata pine showed the importance of determining the characteristics of species and EWPs when developing predictive models and maintenance protocols for longer term service life of timber products (Chiniforush et al. 2019). The reported longitudinal diffusion coefficient values for CLT samples made from Norwegian spruce were higher than those for the transverse direction Chiniforush et al. 2019). CLT 2P had

Fig. 12 Liquid and gas permeability data for CLT samples

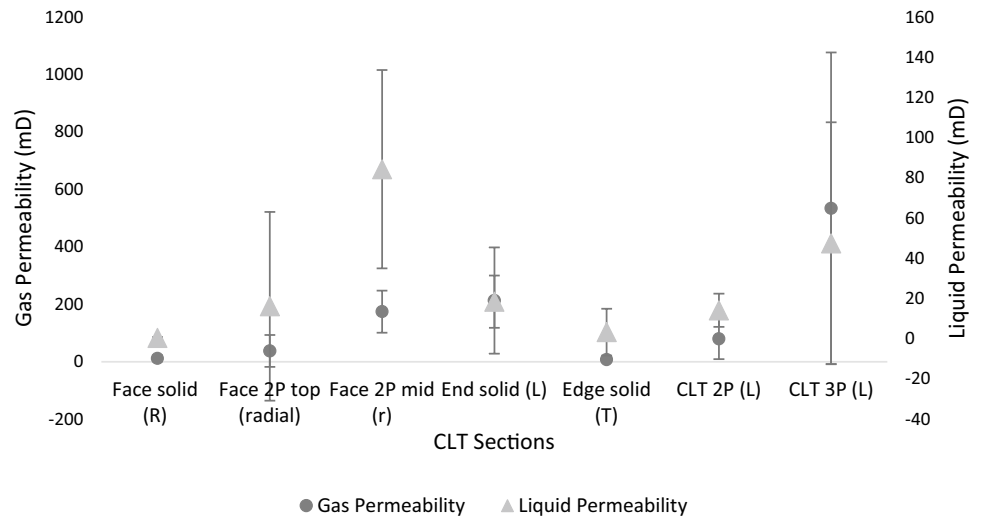


Table 4 Percentage of exposed end grain as well as gas and liquid permeability for CLT 2P samples with no gaps (2P) compared with those for CLT 3P samples with a non-glued edge gap

	Exposed End-grain (%)	Length of edge gap (mm)	Liquid permeability (mD)	Gas permeability (mD)
CLT 2P	54.0 ± 16	–	14.2 ± 0.16	79.94 ± 71
CLT 3P	54.2 ± 17	12.3 ± 3.2	47.5 ± 62.0	471.7 ± 481

± are standard deviations

Table 5 Permeability values determined for LVL samples with two veneer layers and no glue line, one glue line and two glues lines

	Gas permeability (mD)	Liquid permeability (mD)
1 Glue line	28.8 ± 17.3	1.21 ± 1.1
2 Glue lines	20.43 ± 13.3	0.63 ± 1.1
No glue line	145.6 ± 57.0	23.1 ± 11.7

± are standard deviations

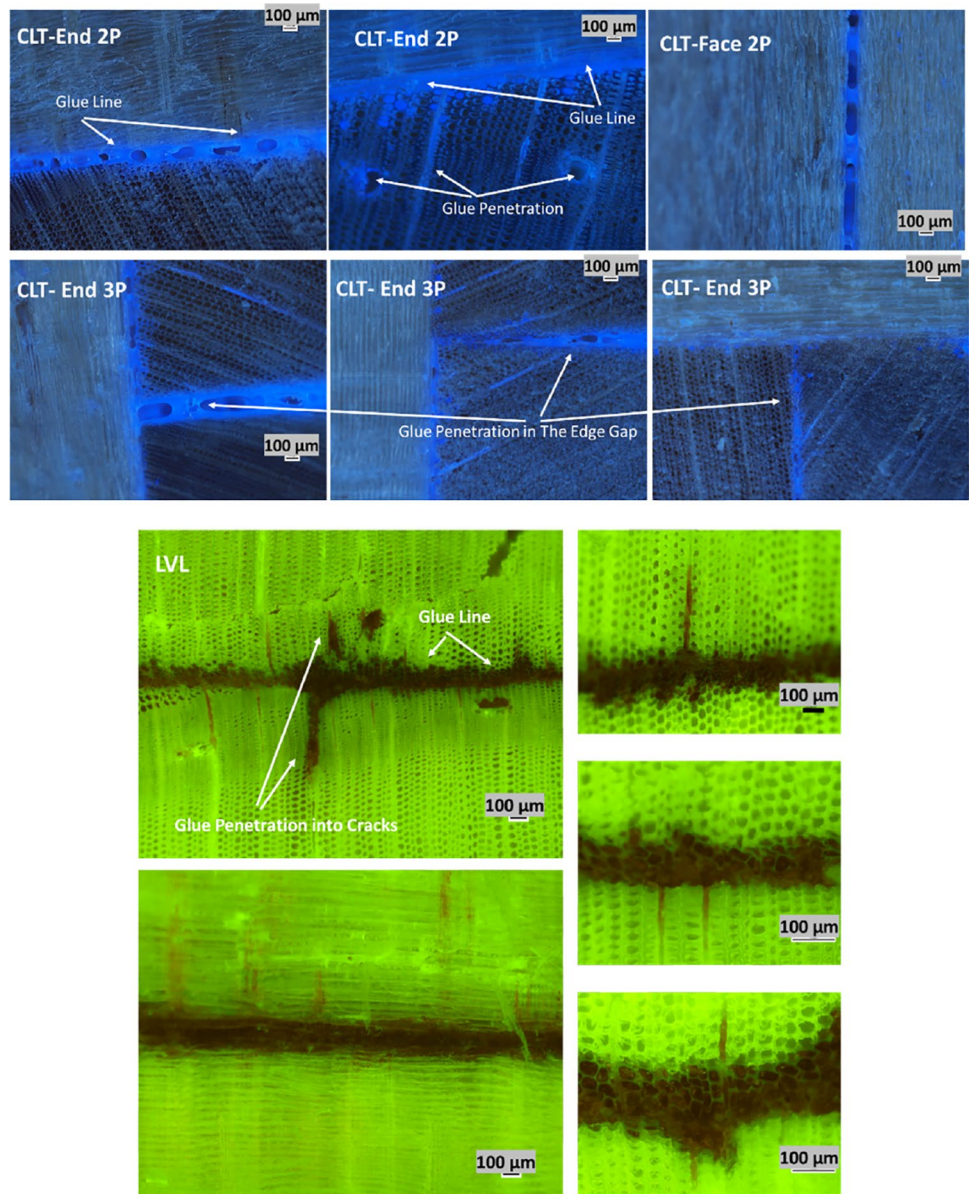
the highest longitudinal diffusion coefficient compared to the other CLT samples (Table 6). CLT 2P diffusion coefficients also had the highest variability, which could be due to the presence of glue lines. The diffusion coefficient determined for CLT 3P in the longitudinal direction was in a similar range to the coefficient in the transverse direction.

4 Conclusion

In this study, the hygroscopic properties of three Australian timber species and two *Pinus* EWPs were investigated. The experimental approach was developed to address the

current gaps in existing knowledge of moisture ingress and egress into LVL and CLT panels. The data collected for all parameters showed the differences between the solid timber sections in three different directions and the effects of glue lines and gaps in composite samples. Porosity values determined from samples of boards and panels showed that as density increases there are variations in percentage of pores in the structure of samples. Solid shining gum had lower porosity values in comparison with southern pine and radiata pine. For CLT samples, porosity values recorded for samples with edge gaps and glue lines were higher than samples with glue lines only. The samples of CLT with glue line (2P) had lower porosity in comparison with radiata pine samples, indicating the effects of glue line in reducing the porosity. LVL samples had high porosity values close to southern pine and radiata samples. The gas and liquid permeability values in radial and tangential directions were lower for shining gum samples in comparison to radiata and southern pine. In the longitudinal direction, southern pine had the highest permeability values and the shining gum values were higher than the radiata pine samples tested. This may have been because of the number of samples tested and the variability within the species structure. Comparison between the composite samples and solid timber samples showed the effects of glue lines and edge gaps in CLT and glue lines and microcracks in LVL samples. Future work is recommended to investigate the influence of different glue types, penetration depth and timber species on the role of the glue line as a moisture barrier in EWP structures. In general, samples with edge gaps and glue lines had higher gas and liquid permeability in comparison with samples with glue lines and no edge gaps. This observation indicates the future need for larger scale modelling and investigation of edge gap effects on moisture ingress rate into the structure and the study of the effectiveness of

Fig. 13 Light microscopic images of CLT and LVL showing glue penetration from the glue lines as well as the gap in non-edge-sealed CLT



using a water membrane or weather barriers to minimise the moisture uptake.

The edge gaps exposed to increased moisture including high RH or free water (condensation and leaks) could become a pathway for moisture trapping or pooling. It is important that the sections with higher possibility of moisture trapping are considered in design detailing to avoid moisture accumulation during construction and in service life of the elements. Allowing air circulation in areas prone to condensation and appropriate drainage design can reduce

the risk of product degradation and decay development in case of free water exposure. The LVL samples with two glue lines had lower permeability than the samples with one glue line. It is important to investigate the effects of glue type, glue line thickness and the number of glue lines on moisture movement, moisture uptake and drying in LVL samples.

The data collected for diffusivity of samples showed the highest diffusion coefficient for CLT 2P section in the end direction. The experimental method used in this study and

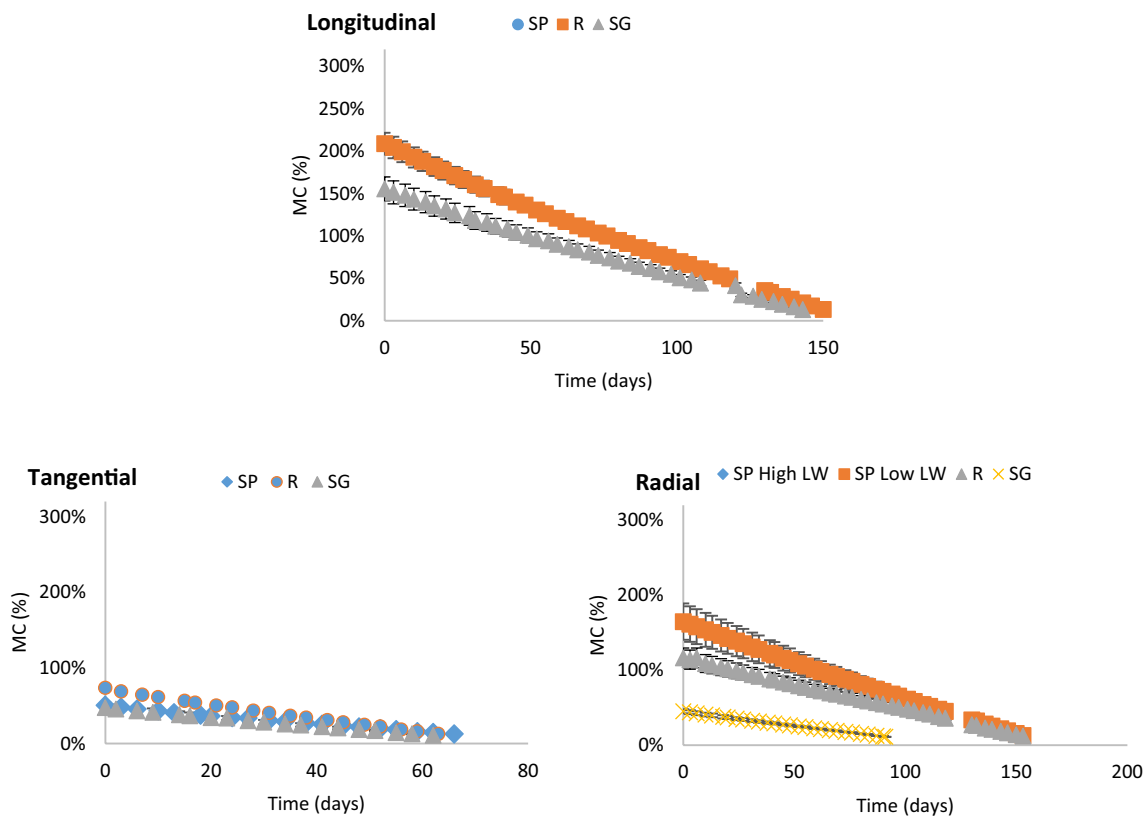


Fig. 14 Effect of longitudinal, radial or tangential orientation on moisture content changes of solid timber samples

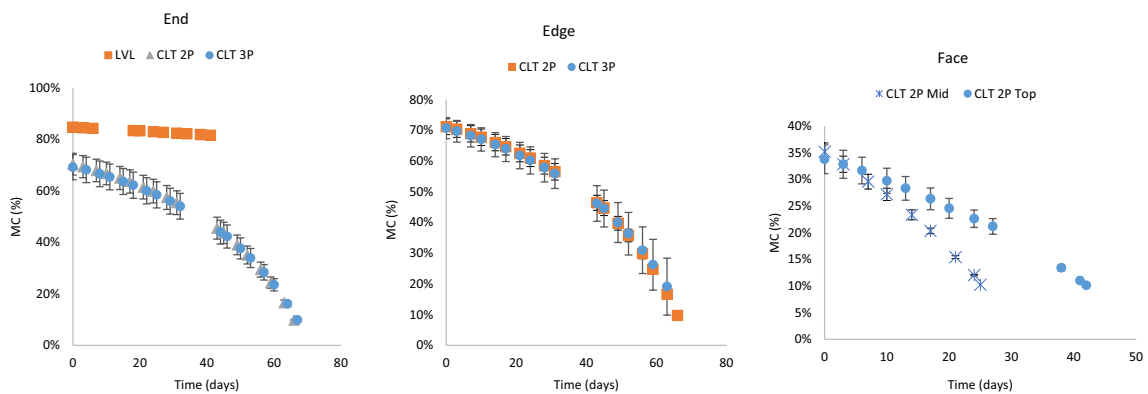


Fig. 15 Effect of diffusion direction on moisture content changes of CLT and LVL samples over time

the data collected for three Australian timber species and EWPs have been used as a part of a larger project focusing on modelling moisture movement in timber products when exposed to free water. The larger project developed

numerical models for solid timber boards, CLT and LVL panels predicting the moisture ingress and egress rates when different environmental conditions applied on different direction of the products.

Fig. 16 Mass loss values recorded for the samples during the exposure to diffusion conditions

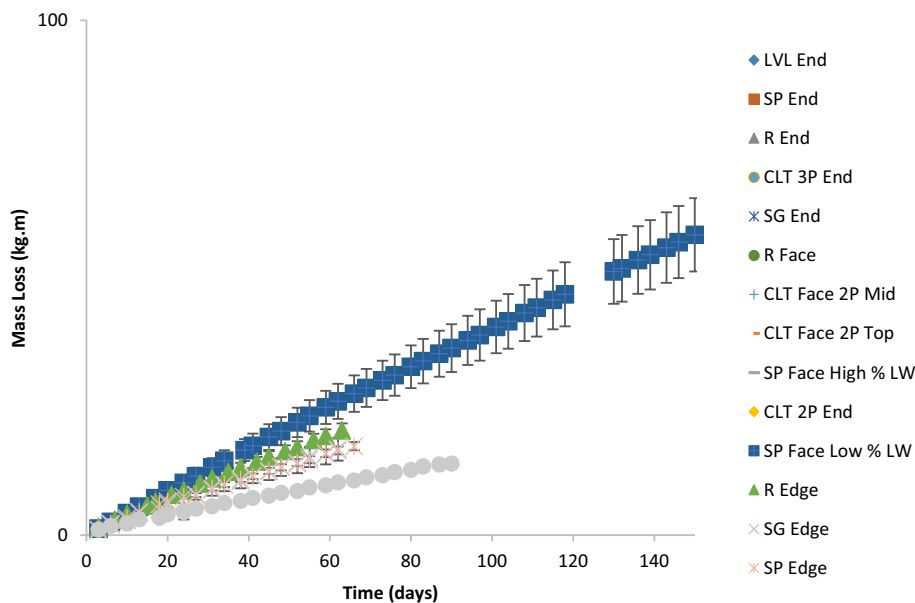


Table 6 Effect of wood orientation on diffusion coefficients and anisotropy ratio for solid wood, CLT or LVL samples

Sample	$D_b (m^2 \cdot s^{-1}) \times 10^{-10}$			Anisotropy ratio		
	L	R	T	D_{bL}/D_{bR}	D_{bL}/D_{bT}	D_{bR}/D_{bT}
Shining Gum	4.17 ± 0.41	0.30 ± 0.01	0.51 ± 0.41	13.99	8.15	0.58
Southern Pine	6.89 ± 0.41	0.68 ± 0.18	0.40 ± 0.03	10.13	17.29	1.71
Radiata Pine	5.52 ± 0.35	0.51 ± 0.05	0.65 ± 0.03	10.74	8.45	0.79
CLT 2P	7.56 ± 9.66	0.95 ± 0.34	2.32 ± 0.27	–	–	–
CLT 3P	2.58 ± 0.60	–	2.49 ± 0.40	–	–	–
LVL	4.89 ± 0.30	–	–	–	–	–

± Values are the standard deviation

Acknowledgements The authors of this paper would like to acknowledge the National Centre for Timber Durability and Design Life and Forest and Wood Products Australia for its support and funding of the project. This work was conducted as part of the project titled “Investigating the effects of moisture ingress on the performance and service life of mass timber panels in Australian climates” funded by the National Centre for Timber Durability and Design Life through Forest and Wood Products Australia. The contribution of the technical team at the Salisbury research facility is gratefully acknowledged.

Author contributions The author confirms that the work presented in this paper is her work and the funding body has been acknowledged in the paper draft.

Funding Open Access funding enabled and organized by CAUL and its Member Institutions.

Data availability Not applicable.

Declarations

Conflict of interest Author declares no conflict of interest in preparing the article.

Open Access This article is licensed under a Creative Commons Attribution 4.0 International License, which permits use, sharing, adaptation, distribution and reproduction in any medium or format, as long as you give appropriate credit to the original author(s) and the source, provide a link to the Creative Commons licence, and indicate if changes were made. The images or other third party material in this article are included in the article's Creative Commons licence, unless indicated otherwise in a credit line to the material. If material is not included in the article's Creative Commons licence and your intended use is not permitted by statutory regulation or exceeds the permitted use, you will need to obtain permission directly from the copyright holder. To view a copy of this licence, visit <http://creativecommons.org/licenses/by/4.0/>.

References

Agoua E, Zohoun S, Perré P (2001) A double climatic chamber used to measure the diffusion coefficient of water in wood in unsteady-state conditions: determination of the best fitting method by numerical simulation. *Int J Heat Mass Transf* 44(19):3731–3744

Australia S (2016) "AS/NZS 1080.3:2000 timber—methods of test, method 3: density", intertek SAI Global Standards Legislation. <https://infostore.saiglobal.com/en-us/standards/>

- AS-NZS-1080-3-2000-117874_SAIG_AS_AS_246811/. Accessed Apr 2022
- Beebe K, Kam-Biron M (2016) Five Ds of moisture management: deflection, drainage, drying, distance, and durable materials. In: Proceedings of the SEAC. Maui, Hawaii, USA. The Engineered Wood Association
- Brischke C, Alfredsen G (2020) Wood-water relationships and their role for wood susceptibility to fungal decay. *Appl Microbiol Biotechnol* 104(9):3781–3795
- Bucklin O, Menges A, Amtsberg F, Drexler H, Rohr A, Krieg OD (2022) Mono-material wood wall: novel building envelope using subtractive manufacturing of timber profiles to improve thermal performance and airtightness of solid wood construction. *Energy Build* 254:111597
- Chang SJ, Kang Y, Yun BY, Yang S, Kim S (2021) Assessment of effect of climate change on hygrothermal performance of cross-laminated timber building envelope with modular construction. *Case Stud Therm Eng* 28:101703
- Chiniforush AA, Valipour H, Akbarnezhad A (2019) Water vapor diffusivity of engineered wood: effect of temperature and moisture content. *Constr Build Mater* 224:1040–1055
- Comstock GL (1970) Directional permeability of softwood. *Wood Fibre Sci* 4:283–289
- Franke B, Franke S, Schiere M, Müller A (2016) Moisture diffusion in wood—experimental and numerical investigations. In: CD-ROM proceedings of the world conference on timber engineering, Vienna, Austria. <https://arbor.bfh.ch/id/eprint/7304>. Accessed Apr 2022
- Friquin KL (2011) Material properties and external factors influencing the charring rate of solid wood and glue-laminated timber. *Fire Mater* 35(5):303–327
- Gaff M, Ruman D, Gašparík M, Štícha V, Boška P (2016) Tensile-shear strength of glued line of laminated veneer lumber. *BioResources* 11(1):1382–1392
- Genstat (2022) "Genstat for Windows" Release 22.1.
- Gereke T, Gustafsson PJ, Persson K, Niemi P (2009a) Experimental and numerical determination of the hygroscopic warping of cross-laminated solid wood panels. *Holzforschung* 63(3):340–347
- Gereke T, Schneider T, Hurst A, Niemi P (2009b) Identification of moisture-induced stresses in cross-laminated wood panels from beech wood (*Fagus sylvatica* L.). *Wood Sci Technol* 43(3–4):301
- Gereke T, Hass P, Niemi P (2010) Moisture-induced stresses and distortions in spruce cross-laminates and composite laminates. *Holzforschung* 64(1):127–133. <https://doi.org/10.1515/hf.2010.003>
- Isaksson T, Brischke C, Thelandersson S (2013) Development of decay performance models for outdoor timber structures. *Mater Struct* 46(7):1209–1225
- Jang E-S, Yuk J-H, Kang C-W (2020) An experimental study on change of gas permeability depending on pore structures in three species (hinoki, Douglas fir, and hemlock) of softwood. *J Wood Sci* 66(1):1–12
- Kukk V, Horta R, Püssa M, Luciani G, Kallakas H, Kalamees T, Kers J (2017) Impact of cracks to the hygrothermal properties of CLT water vapour resistance and air permeability. *Energy Procedia* 132:741–746
- Kukk V, Kalamees T, Kers J (2019a) The effects of production technologies on the air permeability and crack development of cross-laminated timber. *J Build Phys* 43(3):171–186
- Kukk V, Külaots A, Kers J, Kalamees T (2019b) Influence of interior layer properties to moisture dry-out of CLT walls. *Can J Civ Eng*. <https://doi.org/10.1139/cjce-2018-0591>
- Libralato M, De Angelis A, Saro O, Qin M, Rode C (2021a) Effects of considering moisture hysteresis on wood decay risk simulations of building envelopes. *J Build Eng* 42:102444
- Libralato M, De Angelis A, Tornello G, Saro O, D'Agaro P, Cortella G (2021b) Evaluation of multiyear weather data effects on hygrothermal building energy simulations using WUFI Plus. *Energies* 14(21):7157
- Liisma E, Kuus BL, Kukku V, Kalamees T (2019) A case study on the construction of a CLT building without a preliminary roof. *J Sustain Archit Civ Eng* 25(2):53–62
- MacKenzie C, Leicester RH, Wang C-H, Foliente GC (2007) Timber service life design guide. Forest & Wood Products Australia Limited
- Manh HT, Redman AL, Van Pham C, Ngoc BD (2022) Mass transfer properties of *Acacia mangium* plantation wood. *Maderas. Ciencia y Tecnología* 24(2):1–12
- Mohd Yusof N, Md Tahir PD, Lee SH, Khan MA, Mohammad Sufian James R (2019) Mechanical and physical properties of cross-laminated timber made from *Acacia mangium* wood as function of adhesive types. *J Wood Sci* 65(1):1–11
- Niklewski J, Isaksson T, Frühwald Hansson E, Thelandersson S (2018) Moisture conditions of rain-exposed glue-laminated timber members: the effect of different detailing. *Wood Mat Sci Eng* 13(3):129–140
- Öberg, J. and E. Wiege (2018). Moisture risks with CLT-panels subjected to outdoor climate during construction: focus on mould and wetting processes. 15 credits Building technology and Design, KTH Vetenskap Och Konst
- Olsson L (2020) Moisture safety in CLT construction without weather protection—case studies, literature review and interviews. In: E3S web of conferences, 12th Nordic symposium on building physics (NSB), Tallinn, Estonia, 2020
- Perré P, Turner IW (1999a) A 3-D version of TransPore: a comprehensive heat and mass transfer computational model for simulating the drying of porous media. *Int J Heat Mass Transf* 42(24):4501–4521
- Perré P, Turner IW (1999b) Transpore: a generic heat and mass transfer computational model for understanding and visualising the drying of porous media. *Drying Technol* 17(7–8):1273–1289
- Popper R, Niemi P, Croptier S (2009) Adsorption and desorption measurements on selected exotic wood species: Analysis with the Hailwood–Horrobin model to describe the sorption hysteresis. *Wood Res*. <https://doi.org/10.3929/ethz-a-006104740>
- Püssa M (2017) The effect of edge bonding to the properties of cross laminated timber. Master, Tallinn University of Technology
- Quesada-Pineda H, Smith R, Berger G, Loferski J (2020) A visual assessment of cross-laminated timber structures in Austria. *Bio-Products Bus* 5:51–62
- Redman AL (2017) Modelling of vacuum drying of Australian hardwood species. Doctorate Queensland University of Technology. <https://era.daf.qld.gov.au/id/eprint/5882/>. Accessed Apr 2022
- Redman AL, Bailleres H, Turner I, Perré P (2012) Mass transfer properties (permeability and mass diffusivity) of four Australian hardwood species. *BioResources* 7(3):3410–3424
- Redman AL, Bailleres H, Turner I, Perré P (2016) Characterisation of wood–water relationships and transverse anatomy and their relationship to drying degrade. *Wood Sci Technol* 50(4):739–757
- Redman AL, Bailleres H, Perré P, Carr E, Turner I (2017) A relevant and robust vacuum-drying model applied to hardwoods. *Wood Sci Technol* 51(4):701–719
- Rivera Ramos J, Espinoza Herrera R, Arteaga D, Cruz de León J, Olmos L (2021) Microstructural analysis of Eucalyptus nitens wood through computed microtomography. *Wood Mat Sci Eng* 16(5):344–357
- Schmidt E, Riggio M (2019) Monitoring moisture performance of cross-laminated timber building elements during construction. *Buildings* 9(6):144
- Schmidt EL, Riggio M, Barbosa AR, Mugabo I (2019) Environmental response of a CLT floor panel: lessons for moisture management and monitoring of mass timber buildings. *Build Environ* 148:609–622

- Shirmohammadi M, Leggate W (2020) Investigating the effects of moisture ingress on the performance and service life of mass timber panels in Australian climates—Experimental testing plan. Q. G. Department of Agriculture and Fisheries.
- Sofi M, Lumantarna E, Hoult R, Mooney M, Mason N, Lu J (2021) Bond strength of GiR in cross-laminated timber: A preliminary study. *Constr Build Mater* 301:123864
- Taghiyari HR, Avramidis S (2019) Specific gas permeability of normal and nanosilver-impregnated solid wood species as influenced by heat-treatment. *Maderas. Ciencia y Tecnología* 21(1):89–96
- Tanaka T, Avramidis S, Shida S (2010) A preliminary study on ultrasonic treatment effect on transverse wood permeability. *Maderas. Ciencia y Tecnología* 12(1):3–9
- Tibebu D (2021) Fractal modeling of moisture diffusion in wood. Doctor of Philosophy - PhD, University of British Columbia. <https://open.library.ubc.ca/soa/cIRcle/collections/ubctheses/24/items/1.0406072>. Accessed Apr 2022
- Tumer I, Perré P (1995) A comparison of the drying simulation codes TRANSPORE and WOOD2D which are used for the modelling of two-dimensional wood drying processes. *Drying Technol* 13(3):695–735
- Turner IW (1996) A two-dimensional orthotropic model for simulating wood drying processes. *Appl Math Model* 20(1):60–81
- Viitanen H, Toratti T, Makkonen L, Peuhkuri R, Ojanen T, Ruokolainen L, Räsänen J (2010) Towards modelling of decay risk of wooden materials. *Eur J Wood Prod* 68:303–313
- Viitaneu H (1994) Factors affecting the development of mould and brown rot decay in wooden material and wooden structures: effect of humidity, temperature and exposure time. *Mater Struct* 27(1994):483–493
- Viitaneu H (1998) Factors affecting the development of mould and brown rot decay in wooden material and wooden structures: Effect of humidity, temperature and exposure time. Sveriges Lantbruksuniversitet, Sweden
- Wang L, Ge H (2016) Hygrothermal performance of cross-laminated timber wall assemblies: a stochastic approach. *Build Environ* 97:11–25

Publisher's Note Springer Nature remains neutral with regard to jurisdictional claims in published maps and institutional affiliations.